Electronic Supplementary Material (ESI) for Journal of Materials Chemistry A.

Supporting Information

Unique MOF-derived hierarchical MnO_2 nanotubes@NiCo-LDH/CoS_2 nanocages materials as high performance supercapacitor

Xiuhua Wang[1], Feifei Huang[1], Fang Rong[1], Peng He[1], Ronghui Que[1]*, SanPing Jiang[2]**

1 Anhui Key Laboratory of Molecule-Based Materials, The Key Laboratory of Functional Molecular Solids, Ministry of Education, College of Chemistry and Materials Science, Anhui Normal University, Wuhu 241000, China

2 Fuels and Energy Technology Institute & Western Australia School of Mines: Minerals, Energy and Chemical Engineering Curtin University Perth, Western Australia 6102, Australia

List of figures.

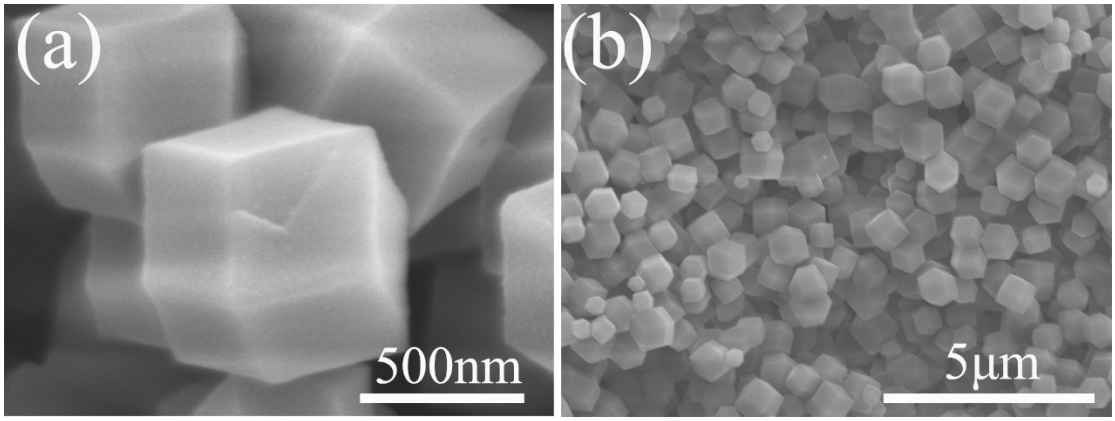

Figure S1. SEM images of the prepared ZIF-67 without the presence of MnO_2 nanotubes (a) in high and (b) in low magnifications.

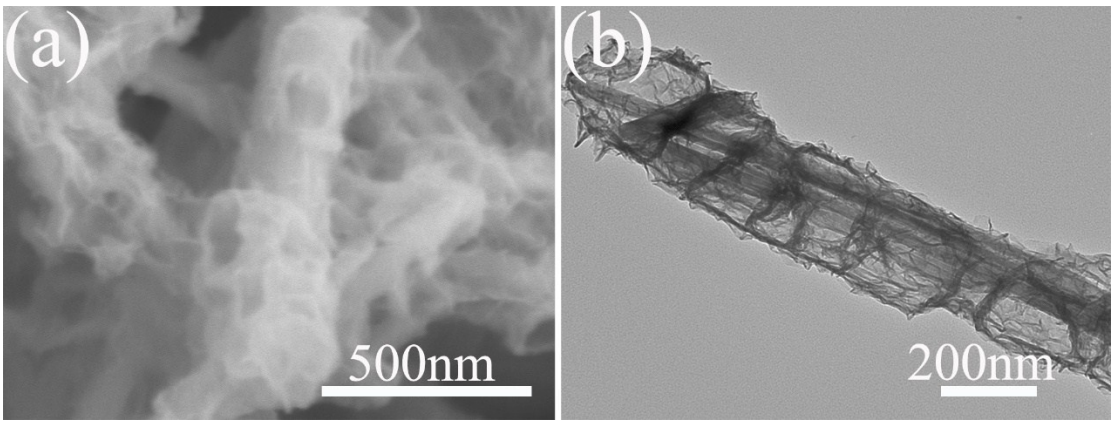

Figure S2. (a) SEM and (b) TEM images of MnO_2@NiCo-LDH-1 (50 mg, 5 h).

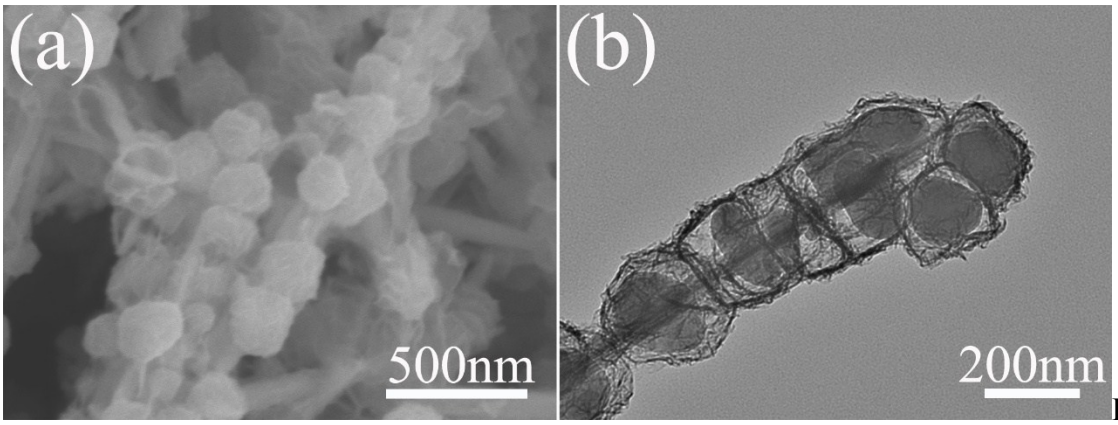

Figure S3. (a) SEM and (b) TEM images of MnO_2@NiCo-LDH-2 (100 mg, 2.5 h).

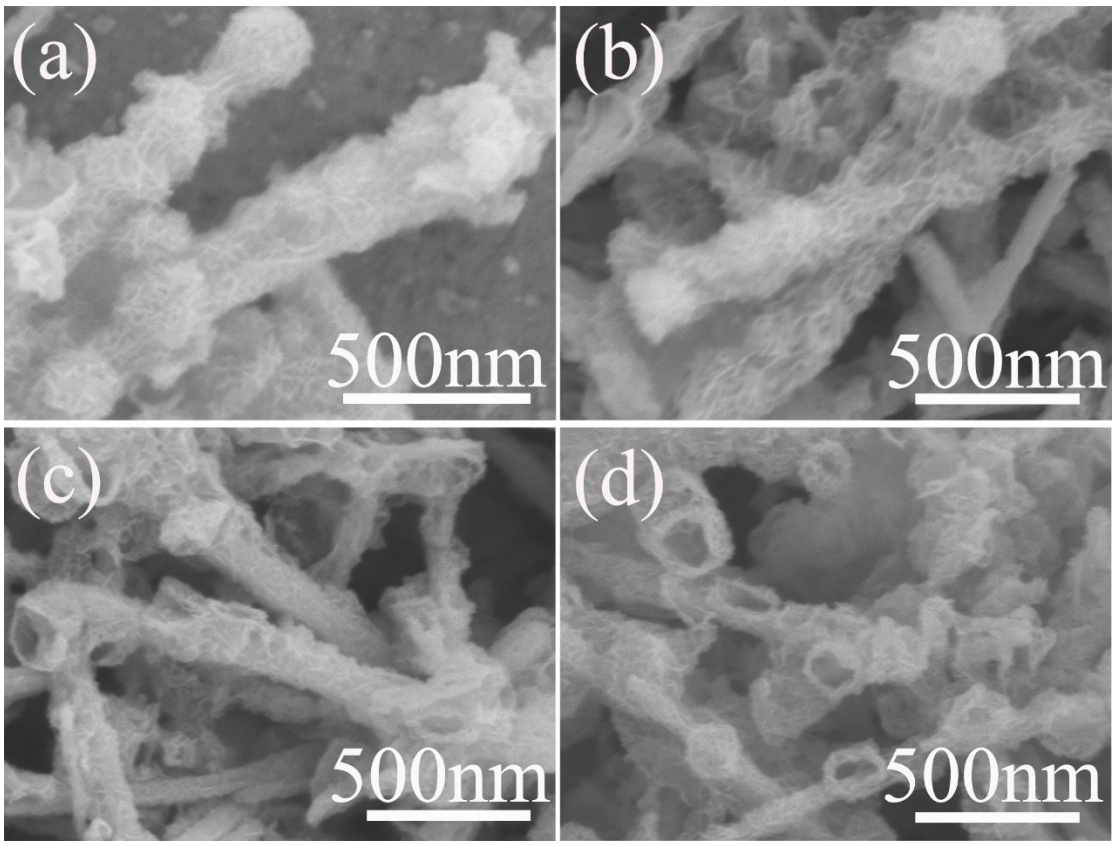

Figure S4. SEM images of (a) MnO_2@NiCo-LDH/CoS_2-1 (15 mg), (b) MnO_2@ NiCo-LDH/CoS_2-2 (30 mg), (c) MnO_2@NiCo-LDH/CoS_2-3 (60 mg) and (d) MnO_2@ NiCo-LDH/CoS_2-4 (120 mg).

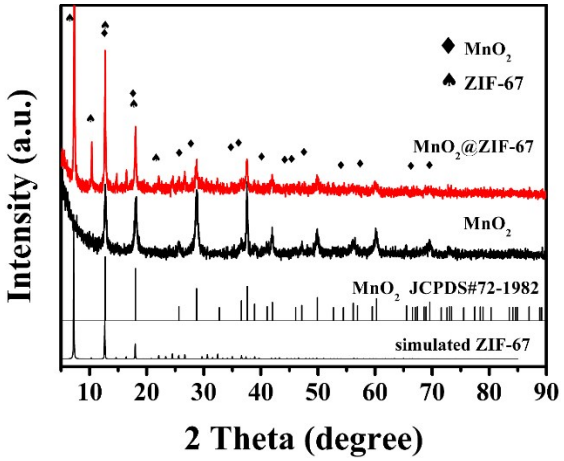

Figure S5. XRD patterns of prepared MnO_2 and MnO_2@ZIF-67.

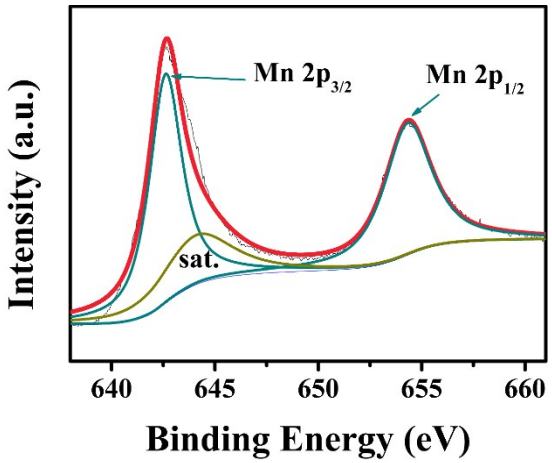

Figure S6. Mn 2p high resolution XPS spectrum for MnO_2@NiCo-LDH/CoS_2.

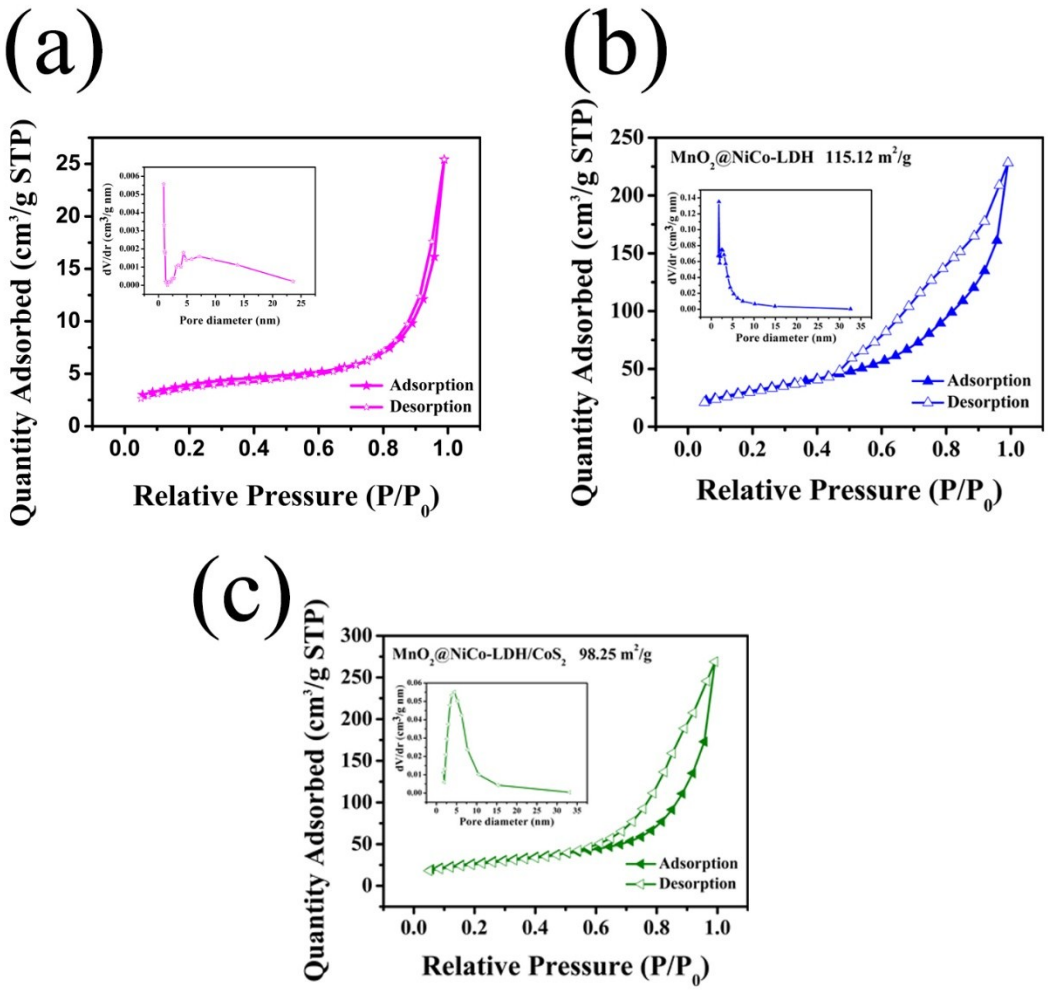

Figure S7. N_2 adsorption/desorption isotherms of (a) MnO_2, (b) MnO_2@NiCo-LDH and (c) MnO_2@NiCo-LDH/CoS_2. The inset is the corresponding pore size distribution.

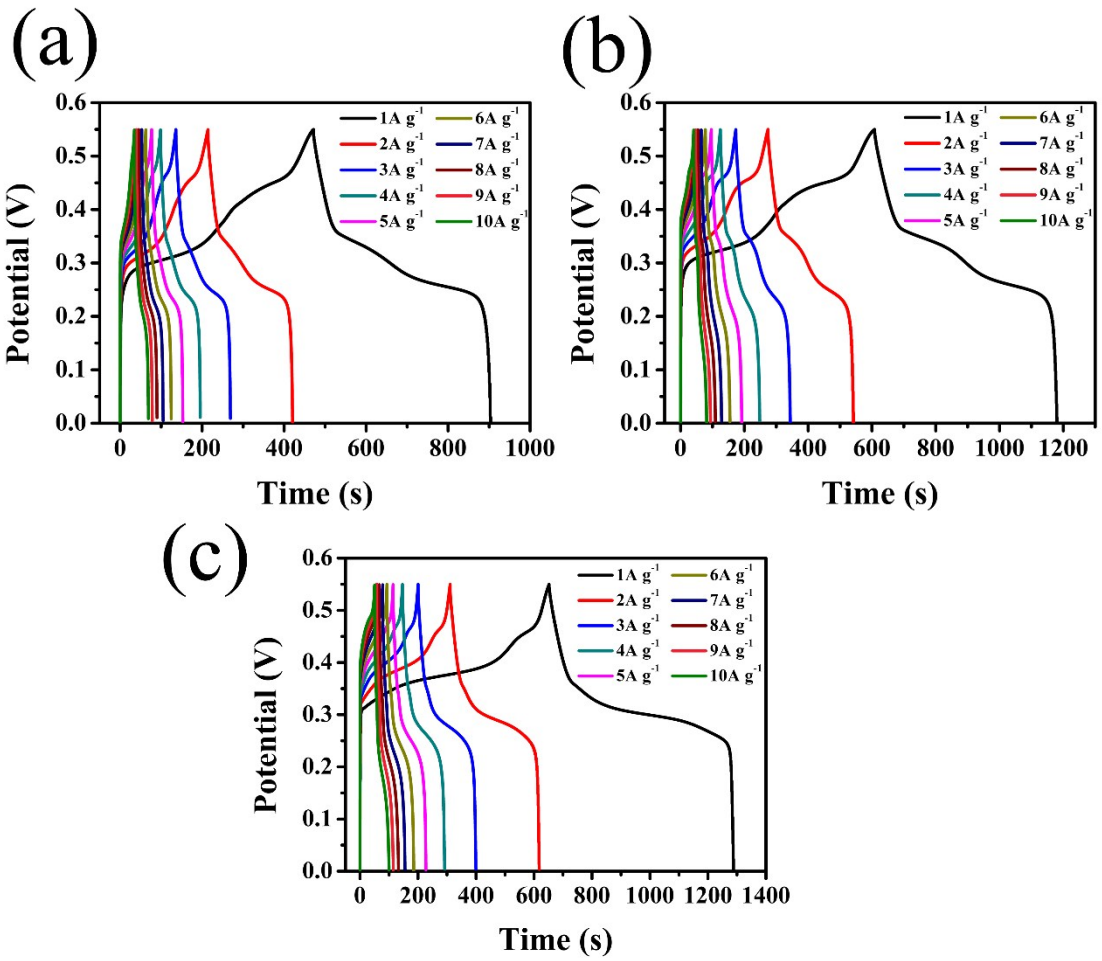

Figure S8. Charge–discharge profiles at various current densities for (a) MnO_2@NiCo-LDH-1 (100 mg, 2.5 h), (b) MnO_2@NiCo-LDH-2 (50 mg, 5 h) and (c) MnO_2@NiCo-LDH (100 mg, 5 h).

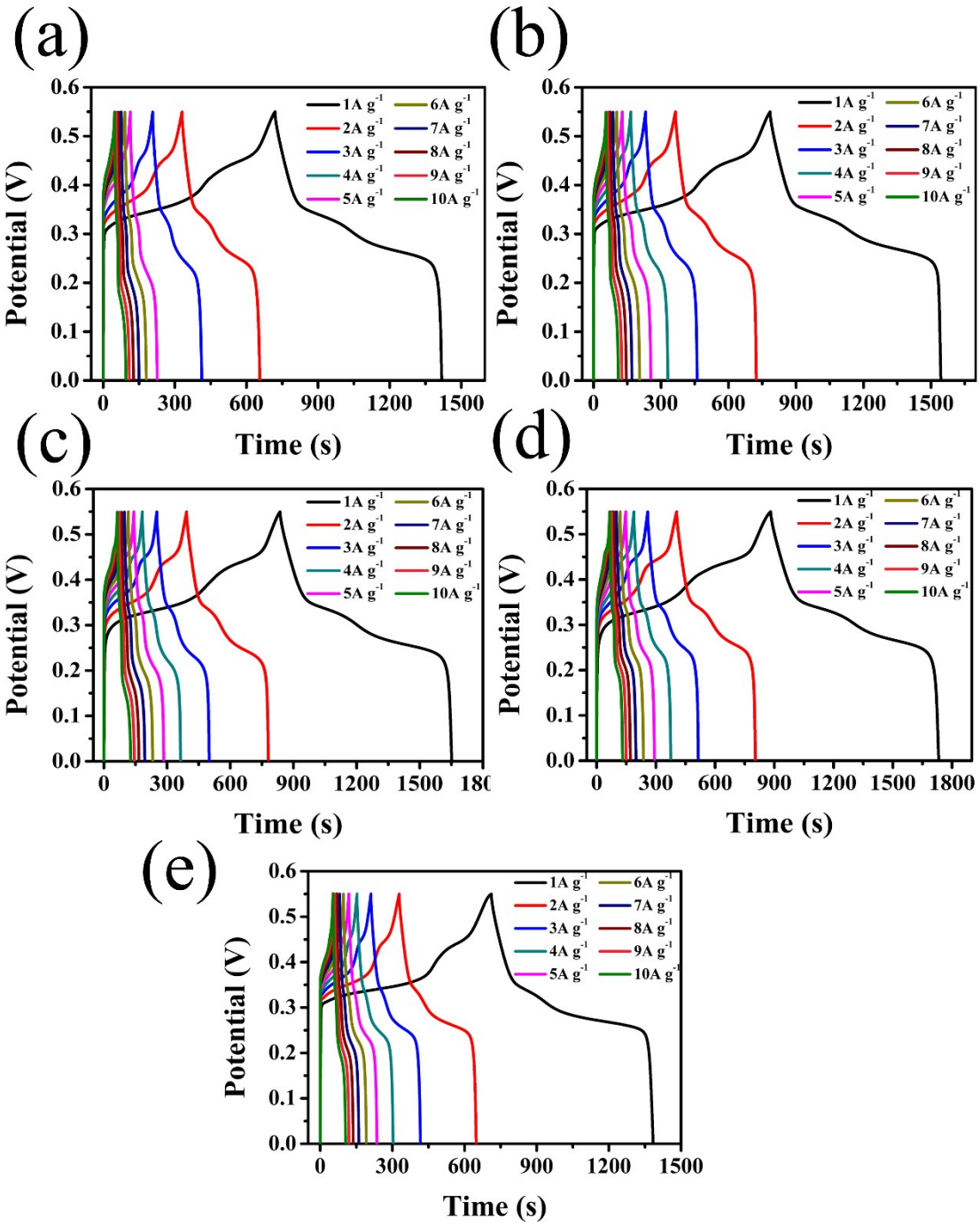

Figure S9. Charge–discharge profiles at various current densities for (a) MnO_2@NiCo-LDH/CoS_2-1 (15 mg), (b) MnO_2@NiCo-LDH/CoS_2-2 (30 mg), (c) MnO_2@NiCo-LDH/CoS_2-3 (60 mg), (d) MnO_2@NiCo-LDH/CoS_2 (90 mg) and (e) MnO_2@NiCo-LDH/CoS_2-4 (120 mg).

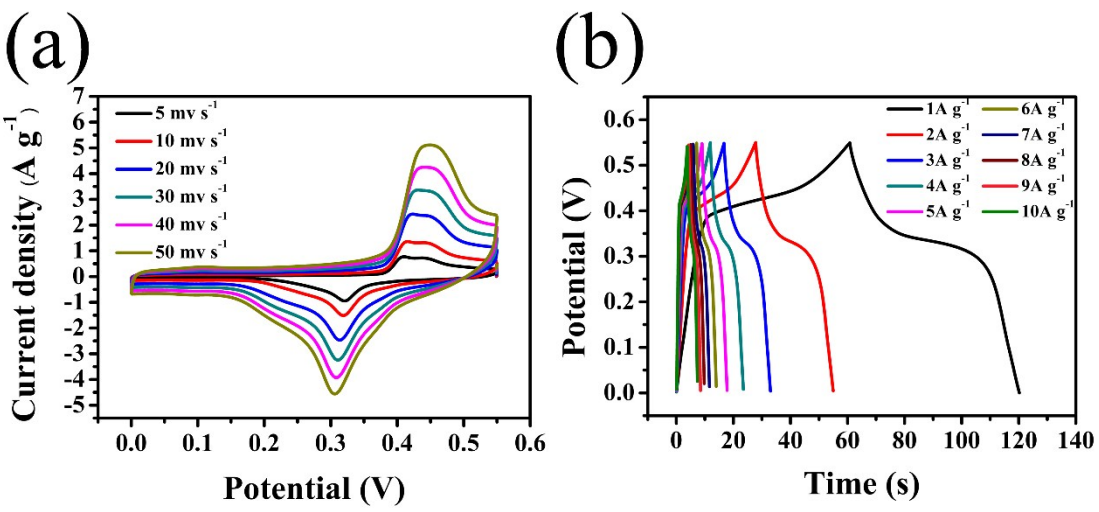

Figure S10. (a) CV curves at various scan rates and (b) charge–discharge profiles at various current densities for MnO_2.

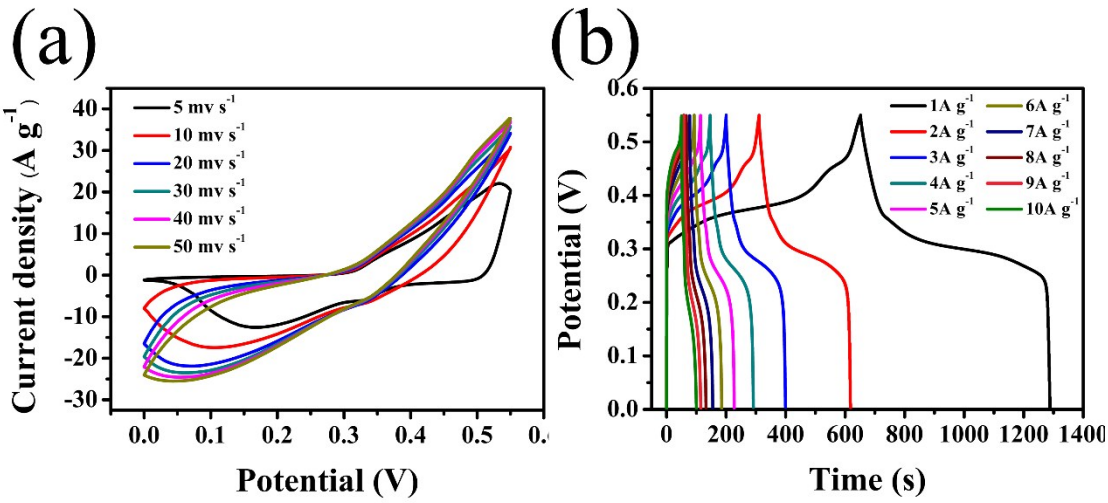

Figure S11. (a) CV curves at various scan rates and (b) charge–discharge profiles at various current densities for MnO_2@NiCo-LDH.

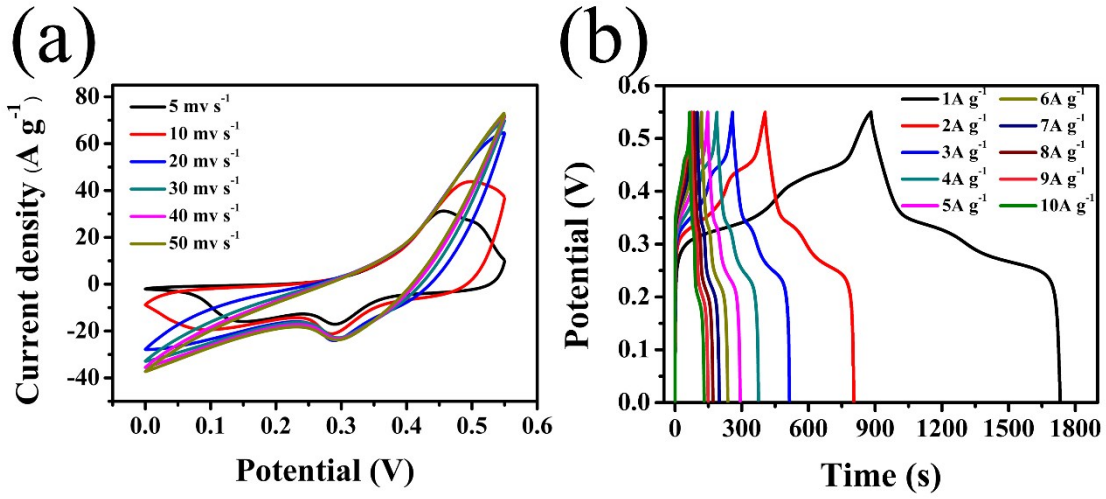

Figure S12. (a) CV curves at various scan rates and (b) charge–discharge profiles at various current densities for MnO_2@NiCo-LDH/CoS_2.

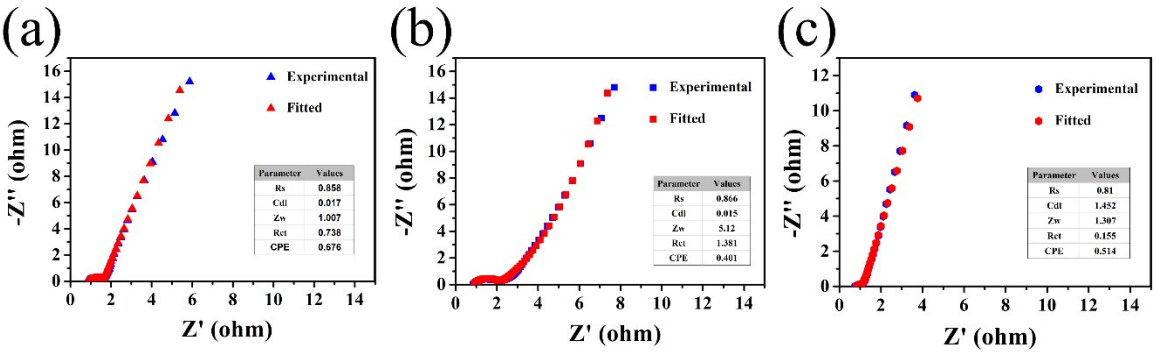

Figure S13. Experimental and simulated Nyquist diagrams of (a) MnO_2, (b) MnO_2@NiCo-LDH and (c) MnO_2@NiCo-LDH/CoS_2. The insert is the corresponding simulation data.

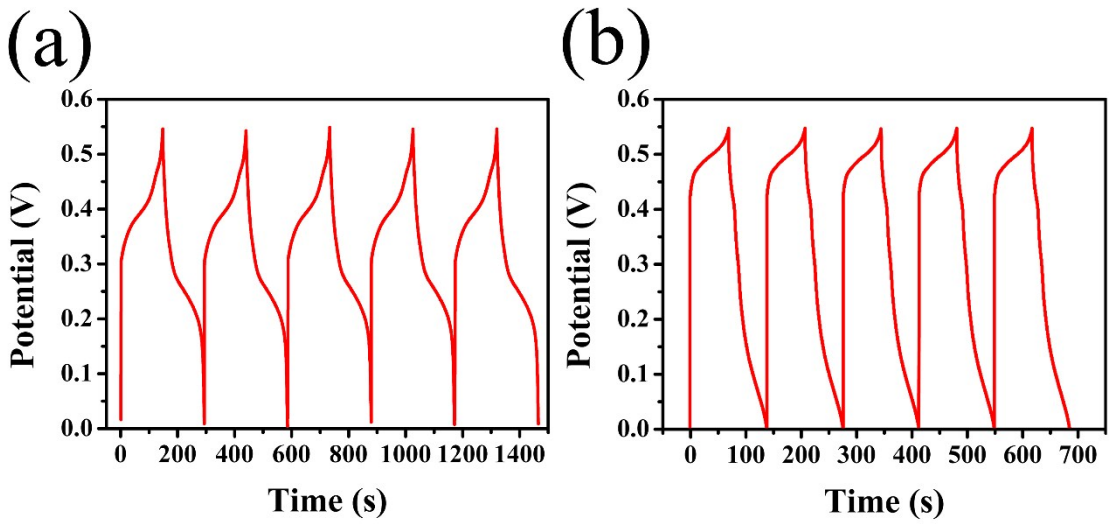

Figure S14. The first (a) and last (b) 5 galvanostatic charge/discharge cycles of MnO_2@NiCo-LDH.

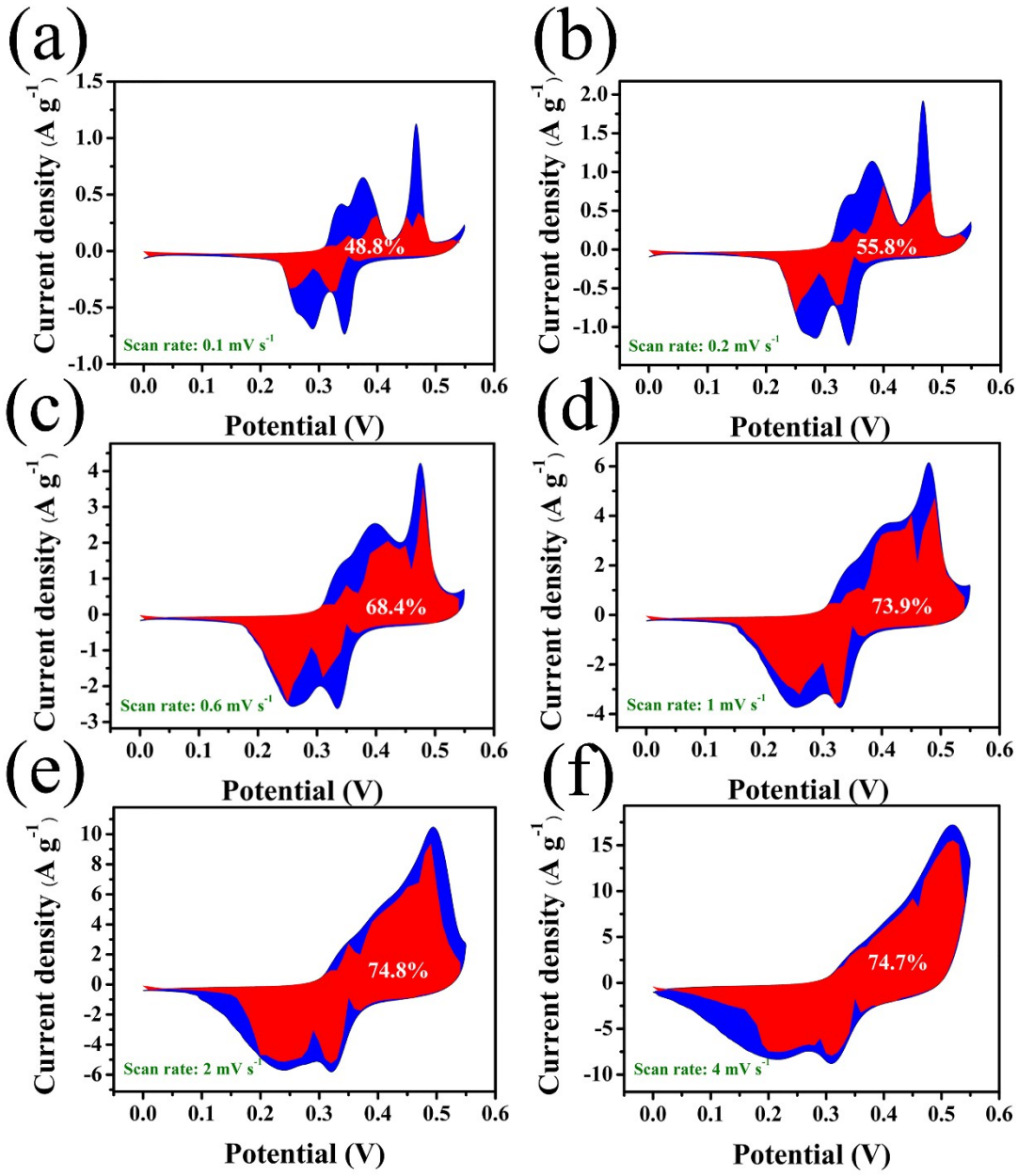

Figure S15. The capacitive contribution to charge storage of MnO_2@NiCo-LDH at different scan rates of (a) 0.1, (b) 0.2, (c) 0.6, (d) 1, (e) 2, and (f) 4 mV s^{-1}.

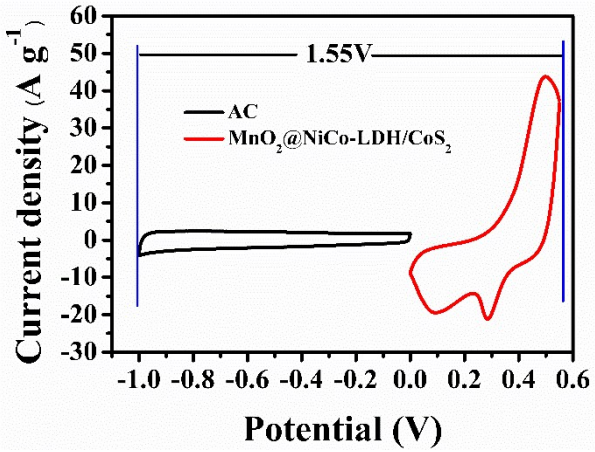

Figure S16. Cyclic voltammograms of AC and MnO_2@NiCo-LDH/CoS_2 in three electrode configurations against SCE electrode showing corresponding operational voltage window.

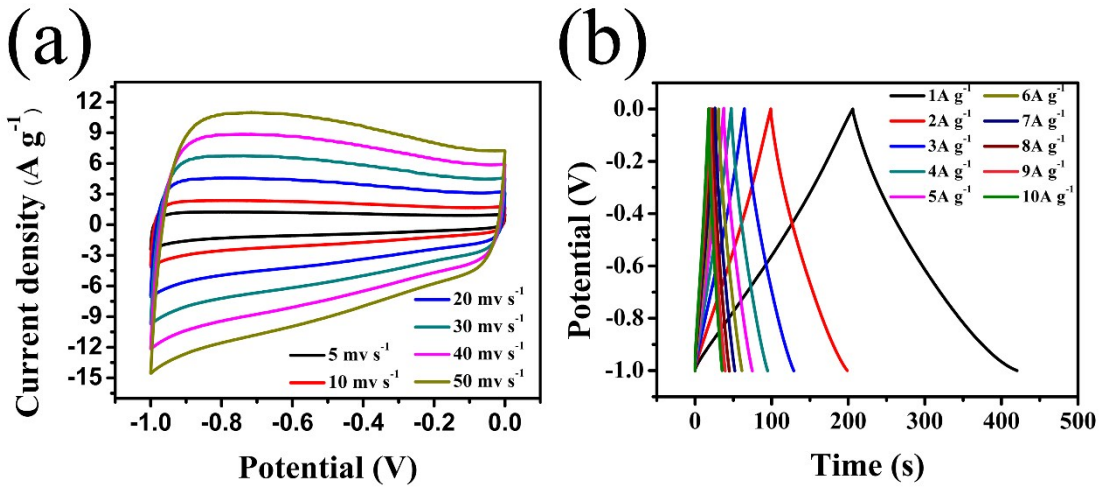

Figure S17. (a) CV curves at various scan rates, (b) charge–discharge profiles at various current densities for AC.

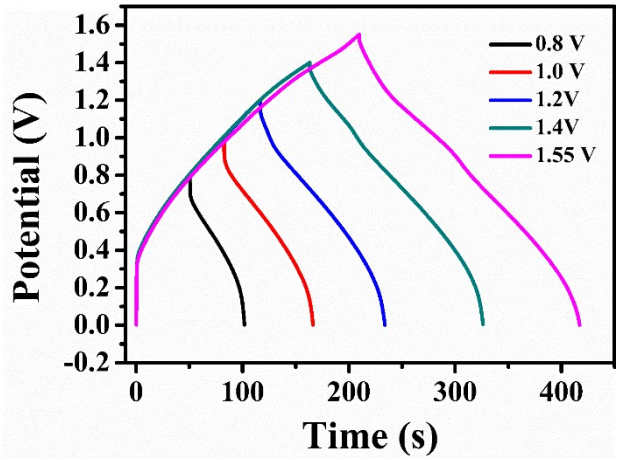

Figure S18. Galvanostatic current charge/discharge curves of MnO_2@NiCo-LDH/CoS_2//AC asymmetric supercapacitor under different potential windows.

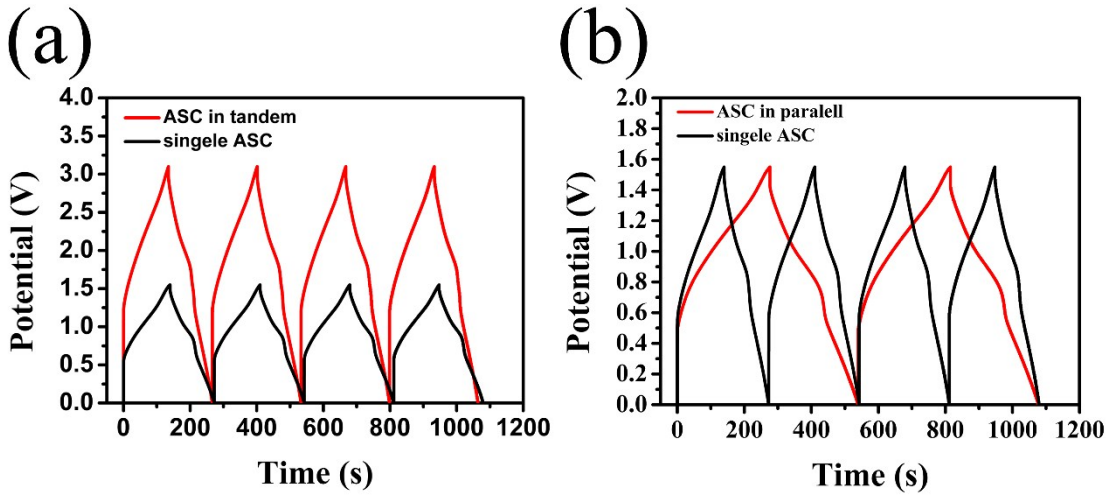

Figure S19 (a) GCD curves of two pieces of MnO_2@NiCo-LDH/CoS_2//AC connected in series, where the working potential doubles from 1.55 V to 3.1 V as compared with one single cell. (b) GCD curves of two pieces of MnO_2@NiCo-LDH/CoS_2//AC connected in parallel, which show twice of the charge/discharge time under the same potential window as compared with one single MnO_2@NiCo-LDH/CoS_2//AC unit.

Table S1. Atomic percentages of the elements in MnO_2@NiCo-LDH/CoS_2 calculated from XPS survey spectra.

Element	Ni	Co	Mn	O	S	C
Atomic %	10.88	5.28	6.44	50.32	7.61	19.46

Table S2. Chemical composition mass percentage of MnO_2@NiCo-LDH/CoS_2 normalized by XPS data.

components	MnO_2	Ni-Co LDH	CoS_2
Weight %	23.82	70.43	5.75

Table S3. BET surface areas, and BJH pore volume and pore radius of the samples.

Sample	SBET (m^2 g^{-1})	Pore Volume (cm^3 g^{-1})	Pore Radius (
MnO_2	13.71	0.037	82.8
MnO_2@NiCo-LDH	115.12	0.355	40.3
MnO_2@NiCo-LDH/CoS_2	98.25	0.417	60.9

Table S4. Comparison of the electrochemical performances of MnO_2@NiCo-LDH/CoS_2 in our work with those reported in the literatures.

Electrode	Specific Capacitance	Capacitance Retention	Mass loading	Reference
MnO_2 @Ni-Co LDH/CoS_2	1547 F g^{-1} at 1 A g^{-1}	76.9% (from 1 A g^{-1} to 10 A g^{-1})	2.0 mg cm^{-2}	Our work
Ni-Co LDH/CNFs	1613 F g^{-1} at of 1 A g^{-1}	68.8% (from 1 A g^{-1} to 10 A g^{-1})	3.13 mg cm^{-2}	10
Ni-Co LDH nanocages	1203 F g^{-1} at of 1 A g^{-1}	78.1% (from 1 A g^{-1} to 10 A g^{-1})	n.a.	16
Co_xS@MnO_2	1635 F g^{-1} at of 1 A g^{-1}	70.9% (from 1 A g^{-1} to 10 A g^{-1})	1.0mg cm^{-2}	18
Co-Co LDH nanocages	1205 F g^{-1} at of 1 A g^{-1}	60.3% (from 1 A g^{-1} to 6.67 A g^{-1})	n.a.	20
Ni-Co nanocages LDH/graphene	1265 F g^{-1} at of 1 A g^{-1}	50.1% (from 1A g^{-1} to 10 A g^{-1})	3.47 mg cm^{-2}	46
rGO/Ag NW/NiAl LDH	1148 F g^{-1} at of 1 A g^{-1}	63.4% (from 1A g^{-1} to 10 A g^{-1})	1.0 mg cm^{-2}	49
MnO_2/LDH/CFs	944 F g^{-1} at of 1 A g^{-1}	71.4% (from 1 A g^{-1} to 10 A g^{-1})	1.2 mg cm^{-2}	50